



SMALL STRAIN DEFORMATION CHARACTERISTICS OF COMPACTED GRAVEL

S. Maqbool¹ and J. Koseki²

ABSTRACT

The effect of compaction on dynamically and statically measured vertical Young's moduli was investigated by performing triaxial and plane strain compression tests using medium scale triaxial and large-scale true triaxial apparatuses. Static and dynamic Young's moduli were evaluated based on results from small cyclic loading and wave velocity measurements respectively. Two series of tests were conducted using Chiba gravel as testing material. In the first series of tests, particles having a diameter larger than 10.5 mm were removed and cylindrical specimens of 10 cm (diameter) x 20 cm (height) having dry densities of 1.76 g/cm³ and 2.00 g/cm³ were prepared. For the static measurement in these specimens, a pair of local deformation transducers (LDTs) (Goto et al. 1991) was set on each specimen. On the other hand, a piezoceramic trigger was set at the top cap and one or two pairs of accelerometers were set on the side of the specimen to generate and receive dynamic wave velocity. In the second series of experiments, the original gradation with $D_{max} = 38$ mm was used to prepare prismatic specimens of 22 cm x 25 cm x 50 cm having dry densities in the range of 1.90 - 2.07 g/cm³. In these tests, three pairs of LDTs were set to measure static vertical Young's moduli and for the dynamic measurement, two accelerometers on one side and two on the other side of the specimen were used. Comparison between statically and dynamically measured Young's moduli was made between test results on these specimens with different dry densities and gradations. As a result of this study, it was found that the difference between the static and dynamic vertical Young's moduli decreased with the increase in the dry density of compacted gravel. Moreover, at relatively low dry density, the relationships between "ratio of static to dynamic wave velocities" and "mean particle size normalized by wave length" observed in this study were consistent with those from previous studies.

Introduction

Heavily compacted gravel has been used in the construction of foundations for huge structures, embankments for dams, roads, railway tracks and airports (Maqbool et al. 2005). Moreover, construction of very large industrial complexes on extensive land reclamation fills and coastal deposits as well as increasing concern about liquefaction due to earthquake loads have caused very high compaction requirements for gravel material. Loose granular deposits are known to undergo large settlements when subjected to vibration arising from machinery, traffic loads and earthquakes. Under static loading, non-uniform density can cause relatively large differential settlement even though the total settlement of the structures on granular material is small. To avoid structural damage due to settlement, it is necessary to compact loose granular material prior to construction. However, these days with the development of new

¹ Associate Professor, Department of Transportation Engineering and Management, University of Engineering and Technology, Lahore, Pakistan. (sajjadmaqbool@hotmail.com)¹

² Prof. Junichi Koseki, Institute of Industrial Science, University of Tokyo, Japan. (koseki@iis.u-tokyo.ac.jp)

techniques, it has become possible to obtain very high dry density in the field, while it has been observed that under working loads, the strain levels within these highly dense deposits as well as in well-designed geotechnical structures are relatively small (Tatsuoka and Kohata, 1995).

In soil mechanics, it is normally assumed that the ground material is a continuum, and that the behavior is linear and recoverable within a very small strain range i.e. less than 10^{-3} % (Tatsuoka and Shibuya, 1992). For the measurement of this “elastic” strain range, the experimental devices have to be very precise and accurate. In this study, very small unloading/reloading cycles were applied at some stress levels, and strains were measured locally using local deformation transducers within a very small strain range at the specimen sides. This method is herein called as “static”. For the “dynamic” measurement in this study, by triggering with pulse wave at some stress levels, the velocity of vertically transmitting compression waves was evaluated from the time difference between the output-1 and output-2 signals as shown in Fig. 2.

In the past, dynamic wave measurements, based on the cross-hole and down-hole methods, have been used for a long time in real construction sites (Stokoe and Hoar, 1978). Recently measurement of wave velocities in the laboratory has also become popular, and researchers have recognized that “static” and “dynamic” properties are no more different from each other (Woods, 1991). Precise static small strain measurements in the laboratory tests have bridged the gap of strain levels between “static” and “dynamic” behavior (Tatsuoka and Shibuya, 1992). Accurate assessment of stiffness is very important to develop several relationships (Lo Presti et al.2006). However, following the pioneer work by Tanaka et al. (2000), AnhDan and Koseki (2002) found that there is still some difference between static and dynamic properties and this difference is not only caused by strain level but also by some other factors like grain size and wavelength. In their preliminary conclusion, the bigger the particle is, the larger the dynamic Young’s modulus becomes as compared with the static one. In this paper, not only the grain size but also the dry densities are varied to check the effect of compaction on Young’s moduli by “dynamic” and “static” measurements.

Testing Material, Equipment and Test Procedures

Specimen Preparation

In this study, two series of tests were conducted in the Koseki Laboratory, at the Institute of Industrial Science, University of Tokyo, Japan. In the first series of tests, medium scale triaxial apparatus was employed. The testing material, as shown in Fig. 1, was Chiba gravel-1 ($D_{max}=10.5$ mm, $D_{50}=3$ mm and $U_c=16$) that was prepared from the original Chiba gravel (Chiba gravel-2 in Figure 1) after removing particles having a diameter larger than 10.5mm. Chiba gravel was originated from crushed sand stone obtained from Kuzuu mountain area, Tochigi Prefecture and could be categorized as sandy gravel. The specimen, as shown in Fig. 2, was cylindrical in shape with dimensions of 10 cm in diameter and 20 cm in height. To measure the vertical stress, σ_1 , a load cell is located just above the top cap inside the triaxial cell in order to eliminate the effects of piston friction (Tatsuoka, 1988).

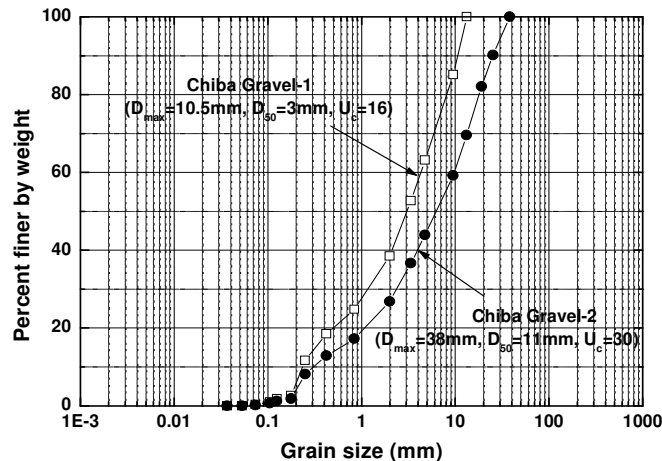


Figure 1. Grain size distribution curve of the test

In this series of tests, two specimens named as G-2 and G-3, were prepared in five layers, and their compaction was made manually by using a compactor having a mass of 5 kg with pre-calibrated number of blows under a free-falling height of 0.45 m that was applied on each layer for achieving the required dry density of 1.92 g/cm³ and 2.00 g/cm³. The membrane used in these tests was 0.5 mm thick. The specimens were partially saturated with water content kept at 5.5%.

In the second series of tests, Chiba gravel-2 ($D_{max}=38$ mm, $D_{50}=11$ mm and $U_c=30$) as shown in Fig. 1, was used as the test material (Maqbool, 2005). Due to larger particle size of this material, a large-scale true triaxial apparatus (AnhDan et al., 2006) was employed. With this apparatus, all three-principal stresses (σ_1 , σ_2 , σ_3) can be controlled independently. The specimen, as shown in Figs. 3 and 4, was rectangular prismatic with dimensions of 50 cm high and 22 cm times 25 cm in cross-section.

To

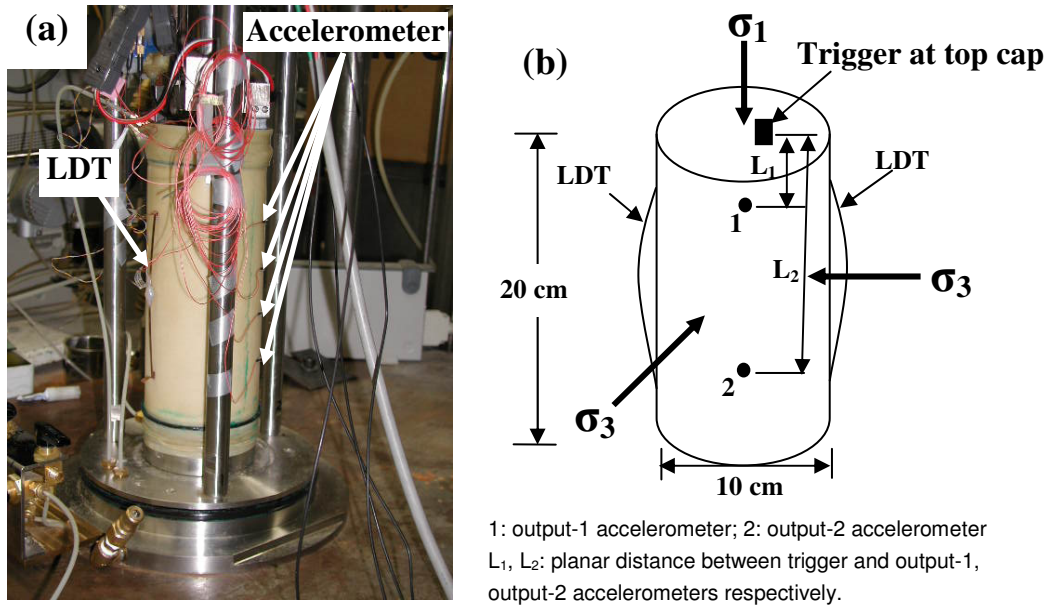


Figure 2. Positioning of LDTs, trigger and accelerometers on medium scale cylindrical specimen; (a) Photo of specimen and (b) Schematic diagram.

measure the vertical stress σ_1 , a load cell is located just above the top cap inside the triaxial cell. The vertical strain ϵ_1 was measured not only externally but also locally with three pairs of vertical local deformation transducers (LDTs). Minor principal stress σ_3 was applied through the cell pressure, which was measured with high capacity differential pressure transducer (HCDPT). The corresponding horizontal strain ϵ_3 was measured with three pairs of horizontal local deformation transducers (LDTs). No lubrication layers were provided at the top and bottom ends of specimen although effect of lubrication layers on Young's moduli has been found insignificant by Maqbool et al. (2006a). In the second series of tests, three partially saturated specimens, named as PS-12, PS-13 and PS-19, were prepared by employing impact loading using steel tamper at water content of 5.5%. Each specimen was prepared in 10-12 layers of equal thickness to obtain overall dry densities in the range of 1.90-2.07 g/cm³. The thickness of each layer was controlled by applying a pre-calibrated number of blows with the tamper mass of 12 kg from a fixed free-falling height of 0.54 m.

Table 1. Testing conditions during the first and second series experiments.

Test	Apparatus	Material	Specimen size	Dry density (g/cm ³)	Accelerometers
G-2	Medium Scale Triaxial	Chiba gravel-1	10cm(dia) x 20 cm (height)	1.76	Type-1 (cylindrical)
G-3				2.00	
PS-12	Large Scale True Triaxial	Chiba gravel-2	22x25x50 cm ³	1.90	Type-2 (box type)
PS-13				2.07	Type-3 (hexagonal)
PS-19				2.02	



Figure 3. Prepared specimen of Chiba gravel for plane strain testing.

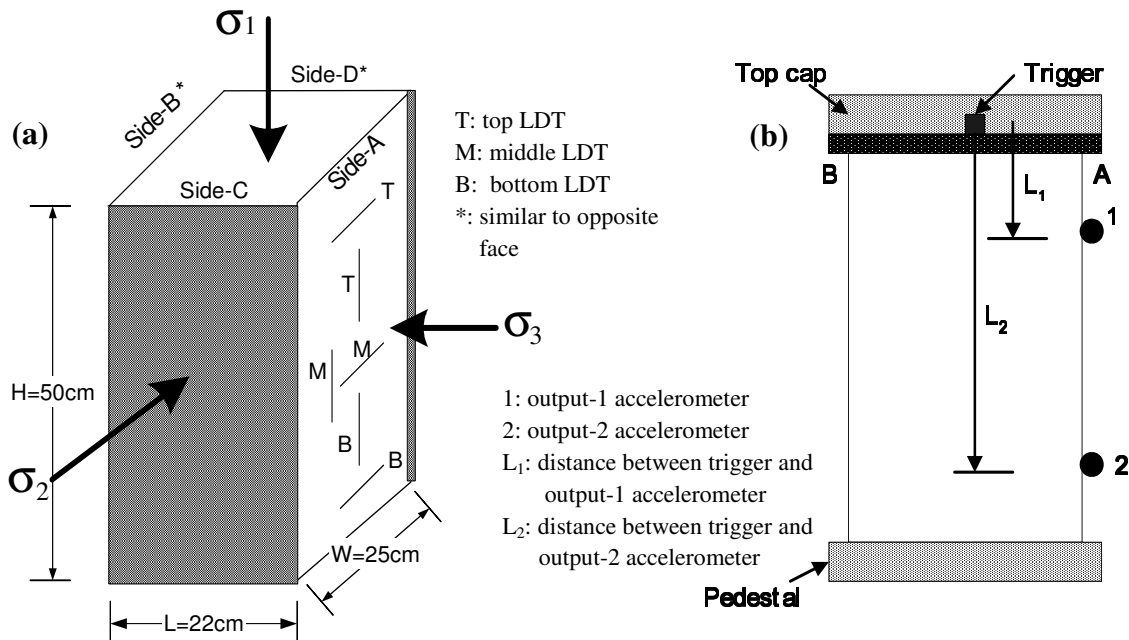


Figure 4. Large scale triaxial specimen; (a) Positioning of LDTs and (b) Location of trigger and accelerometers.

Generating Dynamic Waves

In order to generate dynamic waves, as given in Maqbool et al. (2006b), a special type of wave source (denoted as trigger) was employed. It is a multi-layered piezoelectric actuator made of ceramics (dimensions of 10 mm x 10 mm x 20 mm, mass of 35 gram and natural frequency of 69 kHz, the commercial name is AE 1010D16 of TOKIN company) and a thick steel bar that was bent in a U shape. The actuator was driven by inputting an electric signal of +25 volt in a form of pulse. The mass of each steel bar is 60 grams, and such a large mass was required to provide the reaction force against the dynamic excitation by the piezoelectric actuator. The actuator was put inside the U-shaped steel bar, and they were covered by another steel plate. To generate the vertical compression wave that transmits from the top to the bottom of the specimen, the trigger was glued above the top cap close to the center in the case of the medium scale triaxial apparatus (Figure 2). In the case of the large-scale true triaxial apparatus, as shown in Figure 4b, the trigger was glued inside the top cap.

Receiving Dynamic Waves

As given in Maqbool et al. (2006b), three types of piezoelectric accelerometers were employed to receive dynamic waves. For each test in both series of experiments, the testing conditions are given in Table 1.

Evaluating Vertical Young's Modulus

To evaluate quasi-elastic vertical Young's modulus based on static measurements, at some stress levels, very small unloading/ reloading cycles were applied on the specimen in the vertical direction. Existing data on the deformation properties from cyclic loading tests on dense gravelly soils reported in the literature showed that the behavior at strains less than about 0.001% is nearly elastic (Jiang et al. 1997). Typical stress-strain relationship during a small vertical loading cycle is shown in Figure 5. The increments of the vertical strain and stress were detected with the local deformation transducers (LDTs)

and the internal load cell, respectively. Stress-strain relationships were fitted by a straight line, and the quasi-elastic vertical Young's modulus E_s was evaluated from the slope of the line.

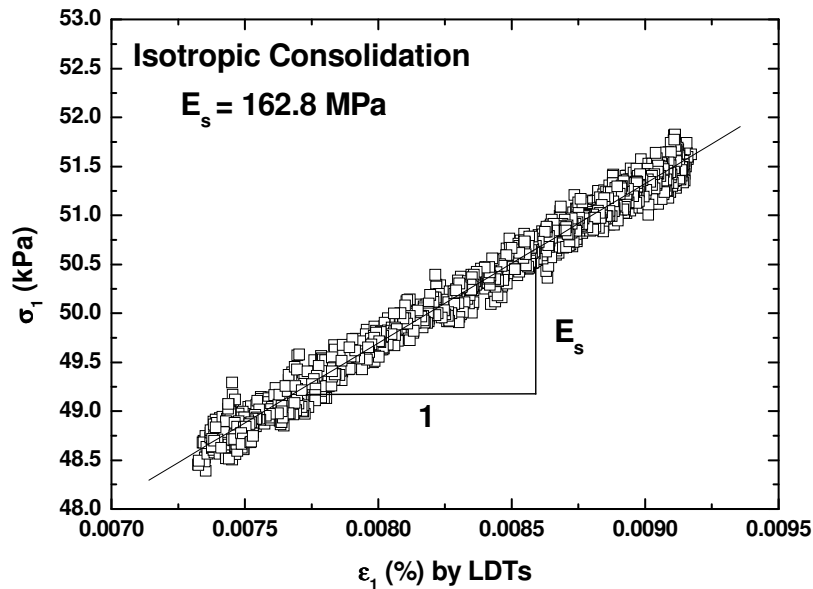


Figure 5. Typical stress-strain relationship during a small vertical loading cycle.

For dynamic measurements, in order to receive a clear signal, AnhDan et al. (2002) suggested to use continuous sinusoidal input for trigger excitation while testing on gravel specimens. In their approach it is sometimes difficult to decide the arrival of the output-2 signal corresponding to the arrival of the corresponding output-1 signal. So in this study by triggering vertically with a single pulse wave at some stress levels, an appropriate wave velocity was evaluated. Moreover, the comparison between single pulse and single sinusoidal wave triggering has been discussed in Maqbool et al. (2006c). As the top cap touched the whole cross-section of the specimen that was with free side boundaries, we assumed that unconstrained compression waves were generated. Its wave velocity V_p is directly related to the small-strain vertical Young's modulus, E_d , of the material by the dynamic measurement as:

$$E_d = \rho V_p^2 \quad (1)$$

where ρ is the mass density of the specimen, and the compression wave velocity V_p was calculated by,

$$V_p = L/t \quad (2)$$

Here t is the travel time of the wave to cover the distance L . The distance L was computed by using the following equations considering the trigger as a planar source to generate the compression waves as shown in Figures 2 and 4b.

$$L = L_2 - L_1 \quad (3)$$

where L_2 and L_1 are the planar distances measured on the side of specimen as shown in Figs. 2 and 4.

All the above parameters could be calculated or measured easily except for the travel time " t ". In many previous researches, a variety of methods to obtain the "correct" travel time have been employed. For example, AnhDan et al. (2002) used the peak-to-peak travel time, while Jovicic et al. (1996) have recommended using the first arrival of the wave. Other researchers have suggested estimation of the travel time from several characteristic points, such as the first rising points, first peaks and first zero-

crossing points in the output-1 and output-2 signals. There are also some researchers who have suggested conducting analysis in the frequency domain to determine the phase angle either indirectly (e.g. Viggiani and Atkinson, 1995) or directly using phase-sensitive detection techniques (e.g. Blewett et al., 1999).

Travel Time Computation

In this study, the wave signals were recorded at two different levels over the specimen using the output-1 and output-2 accelerometers named as “1” and “2” respectively (Figures 2 and 4b). Four different techniques were employed to compute the travel time and compared.

In the first technique, as shown in Figure 6a, “t” was determined using the first peaks of output-1 and output-2 waves. It will be called “peak to peak” travel time technique denoted as “t_{pk}”. In this technique, the observer has to decide the correct peak point. In case of noise-free signal records, the error on decision of “correct peak” are less than in the case of noisy signal records. The authors recommend using this technique for the determination of correct travel time when the data is almost noise free.

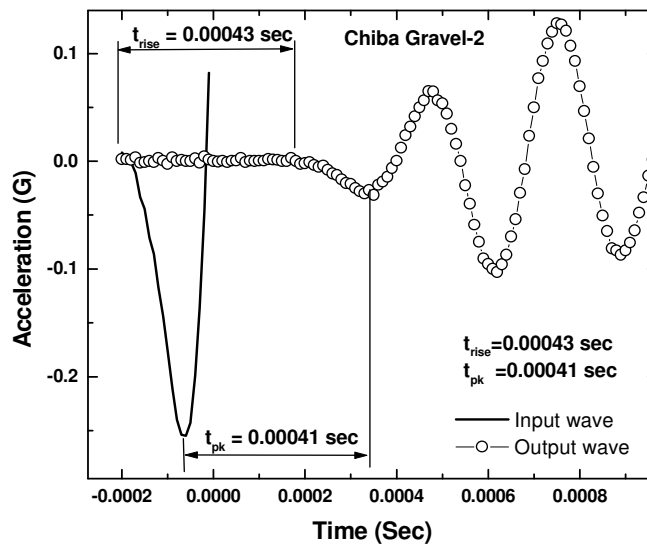


Figure 6. Measurement of travel time “t” of wave using; (a) first rise and first peak techniques (to continue).

In the second technique, as shown in Figure 6a, “t” was computed from the first rising point of the first output-1 wave to the first rising point of the first output-2 wave. It will be called as “first rise to first rise” technique denoted as “t_{rise}”. In this method, a problem lies with the decision of first rising point in both signal records. It may depend on observer’s judgment to decide the correct rising point. After comparing a number of wave signal records obtained in the second series of tests, it was found that t_{rise} was in general by about 5% larger than t_{pk}.

The third technique employed in this study is to use cross-correlation. For this technique, a computer program in PERL language was developed to compute the cross-correlation between the output-1 wave data and the output-2 wave data. The cross-correlation function CC_{xy}(t) is a measure of the degree of correlation of the output-1 and output-2 two signals, X(T) and Y(T), respectively. The analytical expression of the cross-correlation function is,

$$CC_{xy}(t) = \frac{1}{T_r} \int_{T_r} X(T)Y(T+t)dT \quad (4)$$

where T_r is the length of the time records to be matched, and t is the time lag between the signals.

As a first attempt only the first full cycle of the output-1 wave was matched with the full length of the output-2 wave by giving an increment of $10\mu\text{s}$ (equal to data interval) for the time lag, as shown in Figure 6b. The travel time of the wave denoted as " t_{xcorr} " was computed by taking time difference from the starting point of the output-1 wave to the "largest peak" of the cross-correlation. In general the difference between t_{pk} and t_{xcorr} was within 3%.

The last technique employed also the cross-correlation. In this technique, as shown in Figure 6c, instead of matching the first full cycle of the output-1 wave, the first half cycle was matched with the full length of output-2 wave to obtain the cross-correlation. The reason for taking just the first half cycle output-1 wave is to avoid excessive effects of the second half cycle that had larger amplitude than the first one. The travel time obtained by this technique is denoted as " $t_{\text{halfxcorr}}$ ". In general the value of $t_{\text{halfxcorr}}$ was found almost the same as t_{pk} .

Based on the above comparison, it was found that, if the signal record is noise free, then " t_{pk} " is easily employed, while in case of slightly noisy data " $t_{\text{halfxcorr}}$ " should be used to compute travel time of wave. In the following test results, " t_{pk} " was used to compute the travel time. To obtain clear signals of the output-2 waves, stacking technique has been recommended in the literature. Maqbool et al. (2004 and 2006b) found that wave signals became clear when stacking was made for 128 times. Although stacking was not employed in this part of study while it was followed in the later research that will be reported elsewhere.

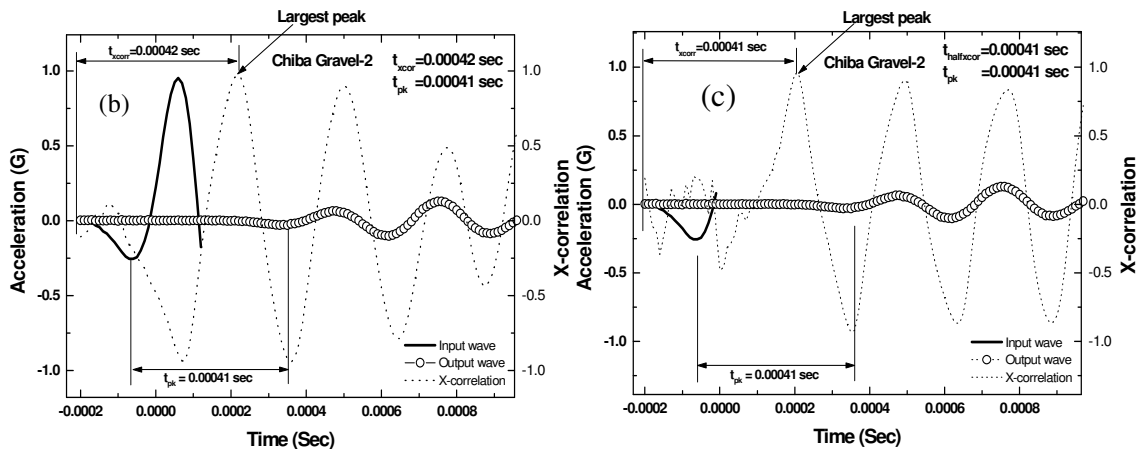


Figure 6(cont). Measurement of travel time " t " of wave using; (b) full input wave cycle cross-correlation technique and (c) half input wave cycle cross-correlation technique.

Test Results and Discussion

Vertical Young's Moduli of Chiba Gravel-1

The specimens were subjected to isotropic consolidation. At various stress levels, compression waves were generated while keeping the stress states constant, followed by application of small vertical unload-reload cycles in order to evaluate the quasi-elastic Young's moduli. In all tests, as typically shown in Figure 5, the strain amplitude during small unloading/reloading cycles was around 0.001%, which is considered to be within the elastic limit. Values of the vertical Young's moduli of Chiba gravel-1, evaluated by the static and dynamic measurements are compared in Figure 7. In the first test on specimen G-2 ($\rho_d = 1.76 \text{ g/cm}^3$), it was observed that the dynamic Young's moduli were almost twice as large as the static Young's moduli at all stress levels. On the other hand, in the second test on a denser specimen (G-3, $\rho_d = 2.00 \text{ g/cm}^3$), the values of the static Young's moduli increased by a factor of about two in G-2. However, the values of the dynamic Young's moduli in G-3 were almost similar to those in G-2.

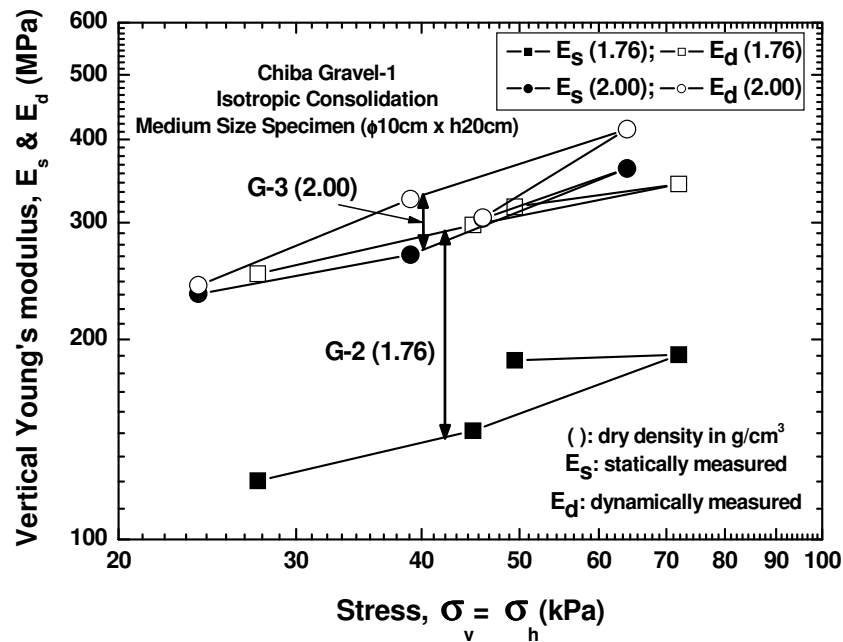


Figure 7. Comparison of vertical Young's moduli during isotropic consolidation for Chiba gravel-1 ($D_{\max} = 10.5 \text{ mm}$)

From these observations, it was found that by the increase of dry density from 1.76 g/cm^3 to 2.00 g/cm^3 , the difference between the static and dynamic Young's moduli was reduced. In order to confirm this behavior, the second series of tests was conducted as given in the following section.

Vertical Young's Moduli of Chiba Gravel-2

The second series of tests on Chiba gravel-2 was conducted using large-scale prismatic specimens. Static and dynamic measurements were made in a similar manner as were employed in the first series of tests. Among three specimens as shown in Figure 8, the first one, named PS-12, was the loosest one having dry density of 1.90 g/cm^3 . With this specimen, the difference between the static and dynamic Young's moduli was larger than in PS-13. In the second test, PS-13 ($\rho_d = 2.07 \text{ g/cm}^3$), the values of the static and dynamic Young's moduli were larger than those in PS-12 though the difference between the static and dynamic Young's moduli became smaller than that in PS-12. In the third test PS-19 ($\rho_d = 2.02 \text{ g/cm}^3$) the values of the static Young's moduli were larger than those in PS-12 while the values of the dynamic Young's moduli were not possible to be measured due to some technical problems. It was only possible to measure dynamic vertical Young's modulus at confining stress of 50 kPa .

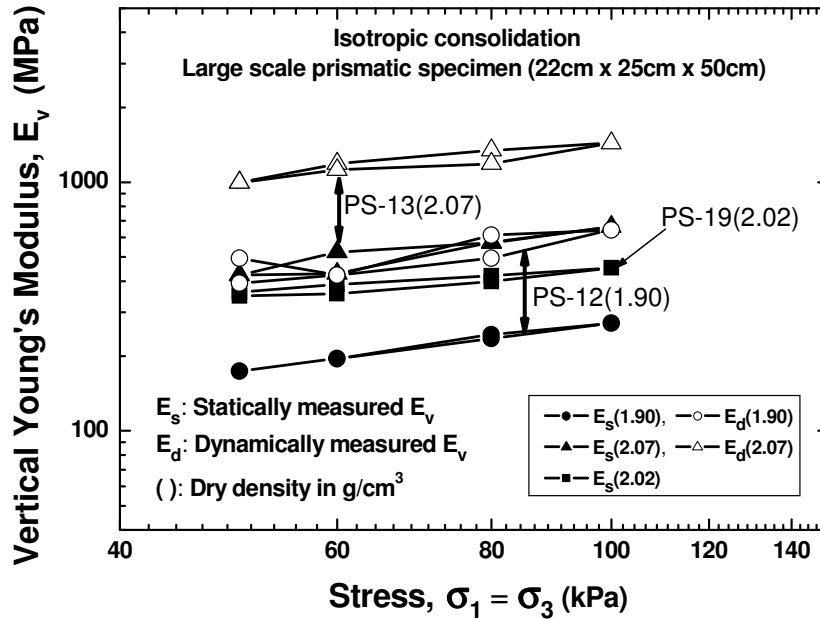


Figure 8. Comparison of vertical Young's moduli during isotropic consolidation for Chiba gravel-2 ($D_{max} = 38$ mm).

The reason for the decrease in difference between E_s and E_d with the increase in dry density would be that in the dynamic measurement unlike the static measurement the wave does not reflect the overall cross-sectional property of the specimen but travels through the shortest path made by interlocking of bigger particles, resulting into larger Young's moduli as compared to those by the static measurement. Detailed study by changing density and compaction level of gravel specimens and its effect on the static and dynamic vertical Young's moduli is in progress to verify such behavior.

Effects of Compaction on Ratio of Static and Dynamic Wave Velocity

It would be natural to assume that different elastic moduli between static and dynamic measurements are affected by the different physical properties of gravelly soils, such as grain size, uniformity coefficient, dry density and wavelength employed in the dynamic measurement. The larger grain size and larger uniformity coefficient of soil would lead to larger structural or microscopic heterogeneity inside the specimen. Tanaka et al. (2000) and AnhDan et al. (2002) reported that the difference between the static and dynamic measurements in terms of wave velocities was affected by the values of $D_{50}/(\lambda/2)$, where λ is the wavelength in the dynamic measurement. In this study, the results obtained from both series of tests having different dry densities and specimen size were converted to V_{cyc}/V_{sv} where V_{cyc} is the wave velocity converted from the static Young's moduli method and V_{sv} is the wave velocity employed in the dynamic measurement. The value of λ was computed using the same definition as used by Tanaka et al. (2000). The test results from this study that are measured at confining stress of 50kPa during isotropic consolidation are shown in Figure 9. At relatively low dry density, the relationships between V_{cyc}/V_{sv} and $D_{50}/(\lambda/2)$ observed in this study were consistent with those from previous studies. It is observed, however, that $D_{50}/(\lambda/2)$ is not the only parameter to affect the values of V_{cyc}/V_{sv} , but the dry density is also an important factor. Both series of tests on Chiba gravel-1 and Chiba gravel-2 specimens showed an increasing trend of V_{cyc}/V_{sv} with the increase in the dry density. It can be concluded that specimens though having similar values of $D_{50}/(\lambda/2)$ can have different V_{cyc}/V_{sv} values depending on their dry density. Even with the increase or decrease in dry density, the wave tends to follow the same path made by stiffer soil particles.

During large earthquakes, the predominant frequency of earthquake motions in the subsurface soils is around 1-2 Hz. At this frequency even for big particle sizes like the gravel tested in the present study, the values of $D_{50}/(\lambda/2)$ would be at largest 0.0005 when effects of non-linearity are neglected. If we assume that the tendency of the difference between the static and dynamic values can be extrapolated from the results above, the difference in the wave velocities between the two methods will be negligibly small, suggesting that the small strain deformation properties evaluated based on the static methods can be employed in the seismic response analysis. The difference will be even smaller for compacted ground as compared to the loose ground. On the other hand, if these properties are evaluated based on in-situ dynamic measurement using shorter wavelengths, due corrections should be made.

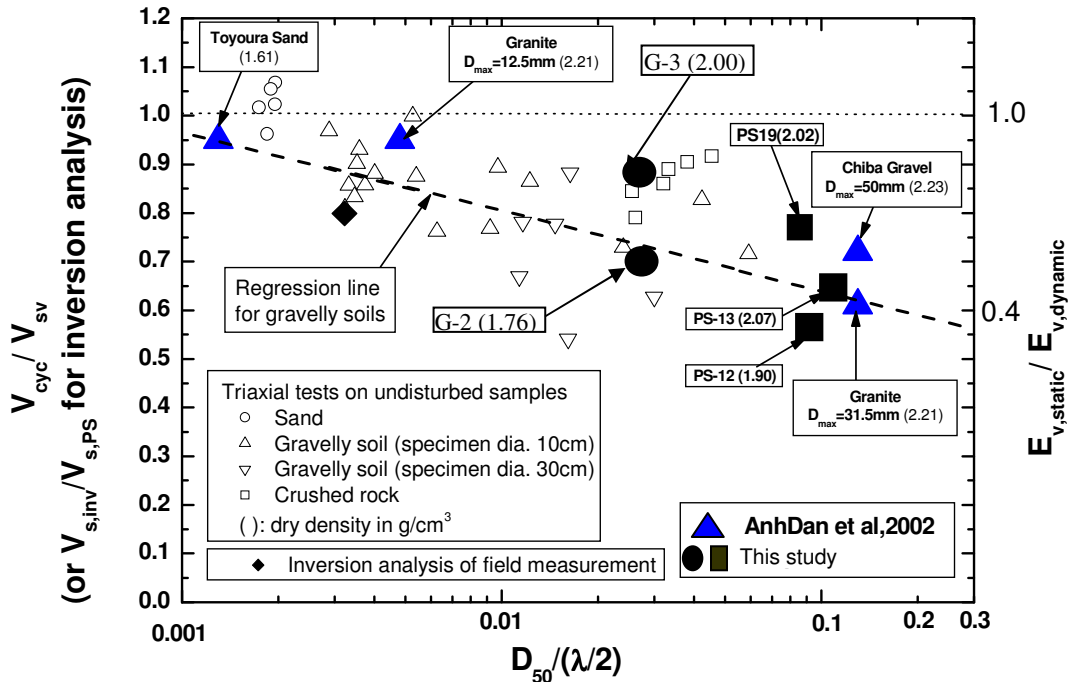


Figure 9. Effects of particle size, wave length and dry density (modified from Tanaka et al. 2000 and AnhDan et al. 2002)

Conclusions

The following conclusions can be drawn from the test results presented in this paper:

- 1- The technique using cross-correlation method by considering “first half cycle of input wave” and full length of output wave signal was found consistent with the peak-to-peak technique for the determination of travel time during wave velocity measurement.
- 2- The difference between the static and dynamic vertical Young’s moduli decreased with the increase in the dry density of compacted gravel. This behavior was observed not only in the medium scale cylindrical specimens but also in the large-scale prismatic specimens. Therefore, if these properties are evaluated based on in-situ dynamic measurement using shorter wavelengths, due corrections should be made.
- 3- At relatively low dry density, the relationships between V_{cyc}/V_{sv} and $D_{50}/(\lambda/2)$ observed in this study were consistent with those from previous studies.

Acknowledgements

The authors would like to thank Mr. Takeshi Sato, Research Support Promotion Member, IIS, the University of Tokyo for providing technical support in conducting experiments at IIS. Thanks to Prof. Fumio Tatsuoka (Tokyo Science University, Japan), Prof. David Muir Wood (Bristol University, U.K.) and

Professor Carlos Santamarina (GeorgiaTech, USA) for their guidance and encouragement during this study. Special acknowledgement to the Ministry of Science, Culture and Education, Japan for providing the first author with financial assistance for his PhD studies in University of Tokyo, Japan.

References

- AnhDan, L.Q., Koseki, J. and Sato, T., 2002. Comparison of Young's moduli of dense sand and gravel measured by dynamic and static methods, *Geotechnical Testing Journal*, Vol.25, No.4, pp.349-368.
- AnhDan, L.Q., Koseki, J. and Sato, T. A, 2006. Large-scale true triaxial apparatus developed for gravel, submitted for possible publication in *Geotechnical Testing Journal: ASTM*.
- Blewett, J., Blewett, I.J. and Woodward, P.K., 1999. Measurement of shear-wave velocity using phase-sensitive detection techniques, *Canadian Geotechnical Journal*, No.36, pp.934-939.
- Goto, S., Tatsuoka, F., Shibuya, S., Kim, Y.S. and Sato, T., 1991. A simple gauge for local small strain measurements in the Laboratory, *Soils and Foundations*, No.1, Vol.31, pp.169-180.
- Jiang, G.L., Tatsuoka, F., Flora, A. and Koseki, J., 1997. Inherent and stress-state-induced anisotropy in very small strain stiffness of a sandy gravel, *Geotechnique*, Vol.47, No.3, pp.509-521.
- Jovicic, V., Coop, M.R., and Simic, M., 1996. Objective criteria for determining G_{max} from bender element tests, *Geotechnique*, Vol.46, No.2, pp.357-362.
- Lo Presti, D., Pallara, O. and Mensi, E. 2006. Characterization of soil deposits for seismic response analysis, Geotechnical Symposium in Rome, Italy.
- Maqbool, S., Sato, T. and Koseki, J., 2004. Measurement of Young's moduli of Toyoura sand by static and dynamic methods using large scale prismatic specimen, Proceedings of the Sixth International Summer Symposium, 2004, JSCE, Saitama, Japan; 233-236.
- Maqbool, S., Koseki, J. and Sato, T., 2005. Effects of large cyclic and creep loading on strength and deformation properties of compacted gravel, Proceedings of the Seventh International Summer Symposium, JSCE, Tokyo, Japan; 187-190.
- Maqbool, S., 2005. Effect of compaction on strength and deformation properties of gravel in triaxial and plane strain compression tests, *PhD thesis*, The University of Tokyo, Japan.
- Maqbool, S., Tsutsumi, T., Koseki, J. and Sato, T., 2006a. Effect of lubrication layers on small strain stiffness of dense Toyoura sand, Proceedings of International Symposium on Geomechanics and Geotechnics of Particulate Media, Ube, Yamaguchi, Japan.
- Maqbool, S., Koseki, J. and Sato, T., 2006b. Effects of compaction on dynamically and statically measured small strain stiffness of gravel, Proceedings of the International Conference on Earthquake Engineering, University of Engineering and Technology, Lahore, Pakistan.
- Maqbool, S., Sato, T. and Koseki, J., 2006c. Dynamically and statically measured small strain stiffness of dense Toyoura sand, Geotechnical Symposium in Roma, Italy.
- Stokoe, K.H., II and Hoar, R. J., 1978. Field measurement of shear wave velocity by crosshole and downhole seismic methods, Proceedings of the Conference on Dynamic Methods in Soil and Rock Mechanics, Karlsruhe, Germany, Vol.III, pp.115-137.
- Tanaka, Y., Kudo, K., Nishi, K., Okamoto, T., Kataoka, T. and Ueshima, T., 2000. Small strain characteristics of soils in Hualien, Taiwan, *Soils and Foundations*, Vol.40, No.3, pp.111-125.

- Tatsuoka, F., 1988. Some recent developments in triaxial testing systems for cohesionless soils, *Advanced Triaxial Testing of Soils and Rock*, STP 977, ASTM, Philadelphia, pp.7-67.
- Tatsuoka, F. and Kohata, Y., 1995. Stiffness of hard soils and soft rocks in engineering applications, *Proceedings of International Symposium on Pre-failure Deformation of Geomaterials*, Vol.2, pp.947-1066.
- Tatsuoka, F. and Shibuya, S., 1992. Deformation characteristics of soils and rocks from field and laboratory tests, *Proc. of 9th Asian Regional Conference of SMFE*, Bangkok, Vol. 2, pp.101-170.
- Viggiani, G. and Atkinson, J.H., 1995. Interpretation of bender element tests, *Geotechnique*, Vol.45, No.1, pp.149-154.
- Woods, R.D., 1991. Field and laboratory determination of soil properties at low and high strains, *Proc. of 2nd International Conference on Recent Advances in Geotechnical Earthquake Engineering and Soil Dynamics*, pp.1727-1741.